Applied Catalysis B: Environmental 192 (2016) 350–356

Contents lists available at ScienceDirect

Applied Catalysis B: Environmental

journal homepage: www.elsevier.com/locate/apcatb

UV-LED assisted catalytic wet peroxide oxidation with a Fe(II)-Fe(III)/activated carbon catalyst

Juan A. Zazo*, Gema Pliego, Patricia García-Muñoz, Jose A. Casas, Juan J. Rodriguez

Chemical Engineering, Faculty of Science, Universidad Autonoma de Madrid, Ctra. de Colmenar km 15, Madrid 28049, Spain

ARTICLE INFO

Article history:
Received 14 January 2016
Received in revised form 30 March 2016
Accepted 6 April 2016
Available online 7 April 2016

Keywords:
CWPO
Fe/AC catalyst
LED
Intensification
Fe(II)-Fe(III)/AC

ABSTRACT

This study assesses the effect of UV LED radiation on the activity and stability of an activated carbon supported iron catalyst in catalytic wet peroxide oxidation (CWPO). Experiments were carried out with a Fe(II)-Fe(III) on activated carbon catalyst, named Fe/AC_M, (4 wt% Fe) in a counter-flow quartz concentric tubular reactor (useful volume: 100 mg/L) surrounded by a commercial LED strip (length: 5 m, 120 LEDs/m, wavelength: 400 nm, irradiance: 10 W/m^2). Phenol was used as target compound at 100 mg/L and the H_2O_2 dose was varied within 100–500 mg/L, the latter corresponding to the theoretical stoichiometric amount. The rest of operating conditions were: $C_{catalyst}$: 500 mg/L, pH_0: 3 and T: 50 °C. UV-LED radiation promotes the reduction of Fe^{3+} to Fe^{2+} on the catalyst surface, increasing the oxidation rate as a result of the higher H_2O_2 decomposition into HO_X• (HO• and HOO•) radicals. Besides, UV-LED radiation easily mineralized oxalic acid, which dramatically reduces the leaching of the active phase (from 17% to less than 4%, without and with irradiation, respectively after 180 min) and increases the life cycle of the catalyst. Thus, a complete H_2O_2 decomposition and more than 98% TOC reduction were reached after 180 min with the stoichiometric amount of H_2O_2. Long-term continuous experiments also confirm the beneficial effects of combining both technologies. TOC reduction above 85% was maintained within the first 100 h on stream with an iron leaching close to 25% of the initial metal load. Longer times on stream led to a slow but continuously decrease of activity probably due to the blockage and/or loss of active sites.

1. Introduction

The increasingly complexity of industrial wastewater, as well as more and more stringent discharge limits, promotes the development of new technologies or the intensification of those already available to remove a wide variety of contaminants, most of them non-biodegradable.

Catalytic wet peroxide oxidation (CWPO) represents an interesting alternative to treat effluents containing recalcitrant pollutants. This advanced oxidation process (AOP) involves the use of H_2O_2 as a source of HO_X• (HO• and HOO•) radicals for the oxidation of organic matter in water at mild working conditions (T: 25–120 °C; P: 1–5 bar).

Besides the efficient consumption of H_2O_2, the key point of CWPO lies on the development of feasible catalysts. Among the several materials proposed, catalysts based on activated carbon as support [1–6] or by itself [7–11], gather suitable properties to be used in this field. In most cases, the catalytic activity is closely related to the presence of iron [5,9], either in the carbon matrix or on the surface. Usually activated carbon-supported catalysts show higher oxidation rates but lower stability, mainly caused by the formation of oxalic acid through the oxidation pathway, promoting the leaching of the metallic active phase, especially in the case of iron, the most commonly used. On the other hand, activated carbon itself or carbon materials containing iron in their structure are more stable but the oxidation rate is markedly lower due to mass transfer limitations.

Most of the efforts to overcome those drawbacks have been focused on improving the anchorage of iron on the catalyst, either modifying the surface itself [12–15] or including iron in the carbon material structure [9,16–18]. However, very little attention has been paid to work under operating conditions that enable the removal of reaction byproducts directly related to iron leaching, like oxalic acid. This compound can be easily mineralized by using UV/Vis light in presence of iron [19,20], since radiation of wavelength below 500 nm provokes the breakdown of iron (III)-oxalate complexes by the following photo-induced, ligand-to metal charge-transfer reaction.

$$[Fe^{3+}(RCOO)^-]^{2+} \xrightarrow{h\nu} Fe^{2+} + CO_2 + R^\bullet \quad (1)$$

* Corresponding author.
E-mail address: juan.zazo@uam.es (J.A. Zazo).

http://dx.doi.org/10.1016/j.apcatb.2016.04.010
0926-3373/

In a previous work [21] we demonstrated the positive effect of Vis-LED radiation upon the degradation of oxalic acid, improving the mineralization achieved by conventional Fenton oxidation. Besides, photoreduction of Fe^{3+} to Fe^{2+} produces additional $HO^{\bullet}$ ($\lambda < 450$ nm) (Eq. (2)), enhancing both the oxidation rate and mineralization.

$$Fe^{3+} + H_2O \xrightarrow{h\nu} Fe^{2+} + HO^{\bullet} + H^{+} \quad (2)$$

The energy consumption of conventional UV lamps is one of the most important costs of photo-Fenton process. Regarding solar light, large areas are needed for its effective application and the associated high cost of installation and the restriction to daylight hours are significant drawbacks [22]. In this sense, light emitting diodes (LEDs), besides providing a reliable and continuous source (unlike solar), are inexpensive and allow high current-to-light conversion efficiencies with low heating.

This work outlines the combination of CWPO and UV LED radiation (λ: 400–405 nm) with the aim of improving the catalytic stability as a consequence of the oxalic acid mineralization and increasing the H_2O_2 yield (ε), defined as the amount of TOC removed (expressed in mg) per unit weight of H_2O_2 fed (expressed in g) [23].

For this purpose, a home-made Fe(II)-Fe(III) on activated carbon catalyst, named Fe/AC_M, was prepared. The presence of both Fe(II) and Fe(III) confers it magnetic properties. An aqueous phenol solution was used as synthetic wastewater, since it is a representative industrial-like wastewater widely used in AOPs studies so that it allows comparison with the results obtained with previous iron on activated carbon catalysts. The magnetic character of the catalyst tested is an additional advantage, since facilitates its separation from the liquid phase. The results were compared with those in the literature in order to remark the positive effect of combining both technologies in terms of catalytic stability and H_2O_2 yield.

2. Materials and methods

2.1. Reactants

Aqueous phenol and H_2O_2 solutions were prepared with phenol (Sigma-Aldrich) and H_2O_2 (30% w/v; Panreac), respectively, at pH 3 using HCl (37% w/v; Panreac). Iron(III) nitrate nonahydrate (98 wt.%) was purchased from Sigma-Aldrich. Working standard solutions of phenol, catechol, resorcinol, hydroquinone, *p*-benzoquinone, maleic acid, acetic acid, formic acid (all obtained from Sigma-Aldrich) and oxalic acid (Panreac) were prepared for equipment calibration. H_2SO_4 (96 wt.%; Panreac), $NaHCO_3$ (Merck), Na_2CO_3 (Panreac), H_3PO_4 (85 wt.%; Sigma-Aldrich) and $TIOSO_4$ (Riedel-deHaën) were also used in the analysis procedures. All reagents were of analytical grade and were used as received without further purification. Milli-Q water was used throughout the work.

2.2. Catalysis preparation

The preparation of the iron on activated carbon (Fe/AC) catalyst was described elsewhere [6,14]. Briefly, it was prepared by incipient wetness impregnation of an activated carbon supplied by Merck (Cod. 102514100; dp: 1.5 mm) with an aqueous solution of iron(III) nitrate nonahydrate in order to obtain a 4% Fe wt.% on the catalyst. Afterwards, the catalyst was calcined at 200 °C for 2 h. Under these conditions, Fe_2O_3 is the main iron specie on the catalyst surface.

The Fe/AC catalyst was further treated under N_2 flow (50 mL/min) at 600 °C for 120 min. Under these conditions, AC reduces a percentage of Fe_2O_3 to Fe_3O_4/FeO [14]. This confers magnetic properties to the catalyst (named Fe/AC_M) that facilitates its recovery from the liquid phase. Besides, the presence of both Fe(II) and Fe(III) on the surface have also influence upon the oxidation rate, mainly during the early oxidation stages.

2.3. Catalyst characterization

The porous structure of Fe/AC_M were characterized from N_2 adsorption/desorption isotherms at 77 K using a Micromeritics Tristar apparatus. The specific surface area (S_{BET}) and the external or non-microporous area (A_{ext}) were calculated by the BET method and t-method, respectively. The total iron content of the catalyst was determined by inductively coupled plasma mass spectrometry (ICP-MS) using an ICP-MS Elan 6000 Perkin-Elmer Sciex instrument. Mössbauer spectroscopy was used to identify the iron species in the catalyst. Mössbauer spectra at room temperature and 77 K were recorded in triangle mode using a conventional spectrometer with $^{57}Co(Rh)$ source. The spectra were analyzed by a non-linear fit using the NORMOS program [24] and the energy calibration was made using a α-Fe (6 μm) foil.

Thermal gravimetric analyses (TGA) were performed on a Metler-Toledo TGA/SDTA 851^e thermobalance in inert atmosphere (N_2 flow: 50 mL/min) from 50 to 900 °C (10 °C/min).

2.4. UV-LED assisted CWPO experiments

UV-LED assisted CWPO runs were performed in a counter-flow quartz concentric tubular reactor (Fig. 1). The aqueous solution (phenol and H_2O_2) and the catalyst are fed throughout the intermediate wall (100 mL useful volume), being continuously recirculated (with a peristaltic pump) to maintain the catalyst suspended. A commercial LED strip (length: 5 m, 120 LEDs/m, wavelength: 400 nm (see Fig. S1 in the 'Supplementary material' Section), irradiance: 10 W/m^2) was placed around the external wall of the reactor.

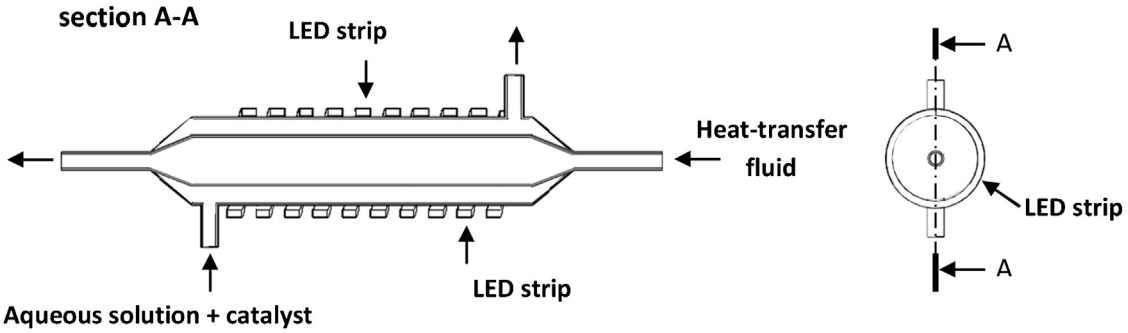

Fig. 1. Scheme of the counter-flow quartz concentric tubular reactor (length: 250 mm, ID external tube: 38 mm; OD internal tube: 30 mm; wall thickness: 1 mm; useful volume: 100 mL).

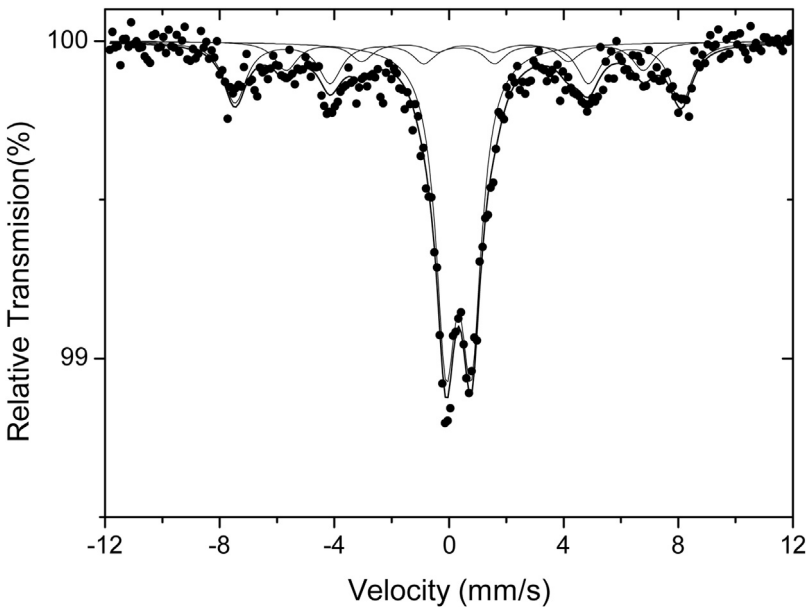

Fig. 2. Room temperature Mössbauer spectra of the Fe/AC_M catalyst.

All the experiments were carried out at 50 °C and an initial pH of 3 with 100 mg/L of aqueous phenol solution and 50 mg of catalyst (particle size <100 μm). The H_2O_2 amount was varied between 20% (100 mg/L) and 100% (500 mg/L) of the theoretical stoichiometric dose for complete mineralization of phenol. All the experiments were carried out by triplicate, being the standard deviation always less than 5%.

Continuous long-term experiments were performed under the same experimental conditions, using always an initial H_2O_2 concentration of 500 mg/L. The inlet and the outlet flow rates (0.5 mL/min) were fixed (using HPLC pumps) to obtain a hydraulic retention time of 200 min. In order to prevent any loss of the catalyst, a porous plate was placed before the outlet.

2.5. Analytical methods

Reaction samples were taken and immediately analyzed after filtration through fiber glass filters (Albet FV-C). Phenol and aromatic intermediates were identified and quantified by means of an Ultra HPLC (Thermo Scientific Ultimate 3000) with a Diode Array detector (Dionex Ultimate 3000). An ion-exclusion column (ROA-Organic Acid H+ (8%), 300 × 7.8 mm, ref: 00H-0138-K0) was used as stationary phase and a 4 mM H_2SO_4 aqueous solution at 1 mL/min as mobile phase. UV detector at 210 nm wavelength was used for phenol, resorcinol, catechol and hydroquinone and at 246 nm for *p*-benzoquinone. Short-chain organic acids were analyzed in an ion chromatograph with chemical suppression (Metrohm 790 IC) using a conductivity detector. A Metrosep A supp 5-250 column (25 cm long, 4 mm diameter) was used as stationary phase and 0.7 mL/min of a 3.2 mM/1 mM aqueous solution of Na_2CO_3 and $NaHCO_3$, respectively, as mobile phase. Total organic carbon was measured using a TOC analyzer (Shimadzu TOC V_{SCH}). The residual H_2O_2 and the iron concentration in the aqueous phase were determined by colorimetric titration with a UV 2100 Simadzu UV/Vis spectrophotometer using the titanium sulfate method [25] and the o-phenantroline method [26], respectively. Ecotoxicity measurements were carried out in triplicate by the Microtox toxicity text, a standard bioassay (ISO 11348-3, 1998). The procedure was describe elsewhere [27].

3. Results and discussion

3.1. Catalyst characterization

Table 1 summarizes the porous structure of fresh Fe/AC_M catalyst. For the sake of comparison, the values of the used catalysts are also included. The BET and external surface area, as well as the pore volumes of the fresh catalyst correspond to a microporous solid with some contribution of mesoporosity. The iron content measured was close to the nominal 4 wt.%.

Hematite and magnetite, as well as metallic iron, were identified by Mössbauer spectroscopy as the iron species in the catalyst. Mössbauer spectra (Fig. 2) was collected at room temperature. The Fe/AC_M catalyst presents a central doublet and a hyperfine magnetic field distribution (sextet). The spectrum of the magnetic

Table 1
Porous structure of fresh and used Fe/AC_M catalyst.

	S_{BET} (m^2/g)	A_{ext} (m^2/g)	V_{micro} (cm^3/g)	V_{meso} (cm^3/g)	Fe (%)
fresh catalyst	950	72	0.38	0.12	4.1
adsorption run	430	86	0.11	0.07	4.0
UV-LED CWPO runs (% stoichiometric H_2O_2)					
20%	360	84	0.10	0.07	3.9
40%	340	78	0.09	0.06	3.8
60%	352	81	0.10	0.07	3.8
80%	346	80	0.10	0.06	3.7
100%	338	84	0.09	0.06	3.7
Long-term continuous experiment					
–	324	97	0.09	0.05	3.1

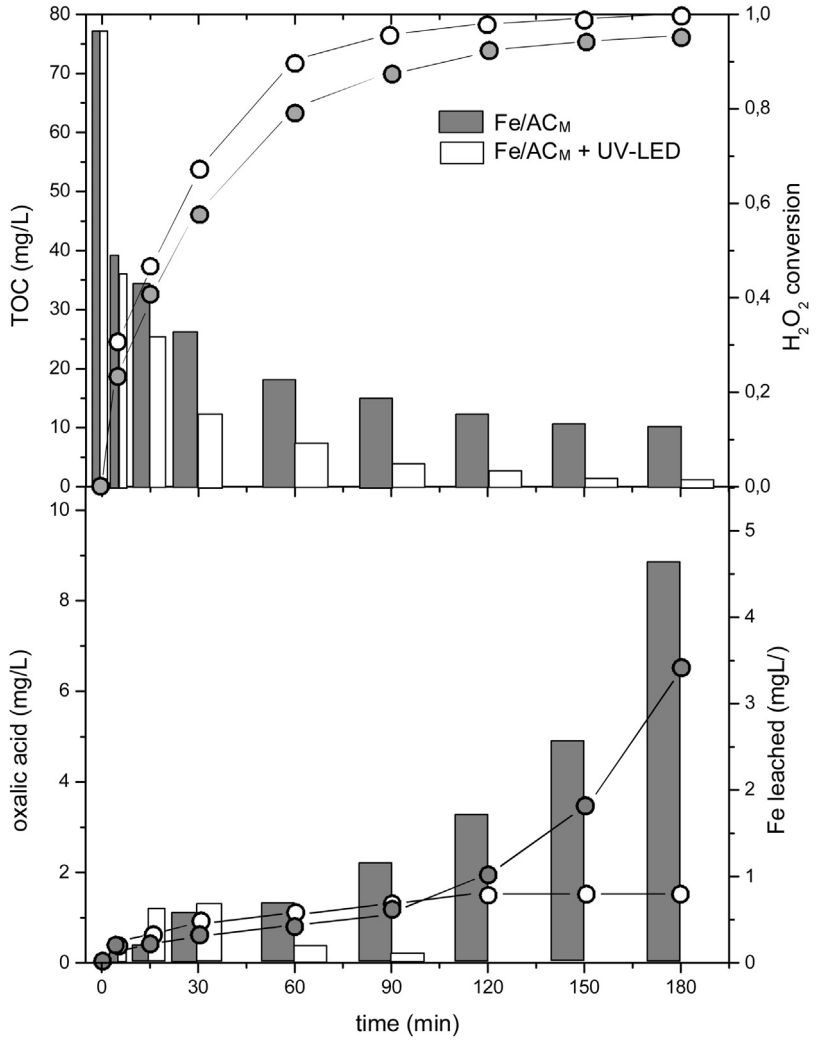

Fig. 3. Time evolution of TOC and oxalic acid (bars), H_2O_2 and Fe leached (symbols) upon CWPO with and without UV-LED radiation. [$C_{phenol,0}$: 100 mg/L, $C_{H2O2,0}$: 500 mg/L, C_{cat}: 500 mg/L, T: 50 °C and pH_0: 3].

catalyst contained three sextets, corresponding to Fe(III) in the tetrahedral positions and Fe(II)/Fe(III) in the octahedral positions of the magnetite, respectively. The third sextet is identified as metallic iron, formed also in the reduction step. The relative amount of this species was below 10%. The central doublet can be identified as iron oxide nanoparticles, Fe_2O_3 or Fe_3O_4, smaller than 10 nm and therefore superparamagnetics.

3.2. CWPO-LED activity

In order to quantify the effect of UV-LED radiation upon the oxidation of phenol (100 mg/L) by CWPO, a set of experiments with and without irradiation were carried out at pH 3, using 500 mg/L of the Fe/AC$_M$ catalyst (Fe 4 wt.%) and the stoichiometric amount of H_2O_2 (500 mg/L). The results are shown in Fig. 3. Also, preliminary photolysis experiments in absence of both, catalyst and H_2O_2, were performed (data not shown), yielding TOC reduction lower than 10% after 180 min reaction time.

As can be seen, UV LED radiation significantly enhances the oxidation rate and the mineralization degree achieved by CWPO. H_2O_2 decomposition rate increases with irradiation, giving rise to higher TOC reduction. Thus, aromatics were completely depleted in the first 15 min (versus up to 120 min without radiation) and the concentration of short-chain organic acids was much lower than those measured in absence of UV LED radiation at similar TOC conversion (see Fig. S2 and Fig. S3 in the 'Supplementary material' Section). This is especially remarkable for oxalic acid, main responsible of the deactivation of Fe/AC catalyst in CWPO [6]. As can be observed in Fig. 3, at a TOC conversion around 85%, oxalic acid concentration in the reaction media decreased from 9 mg/L to around

Table 2
TOC removal and concentrations of reaction byproducts and Fe in the effluent from CWPO with UV-LED radiation at the operating conditions of Fig. 3 (except H_2O_2 concentration).

H_2O_2 dose (% of stoichiometric)	TOC removal (%)	$\Sigma_{aromatics}$ (mg/L)	Σ_{acids} (mg/L)	$Fe_{leached}$ (mg/L)
20	62	18.5	2.3	0.4
40	94	4.1	8.8	0.6
60	95	0	6.1	0.7
80	96	0	4.0	0.8
100	98	0	2.1	0.8

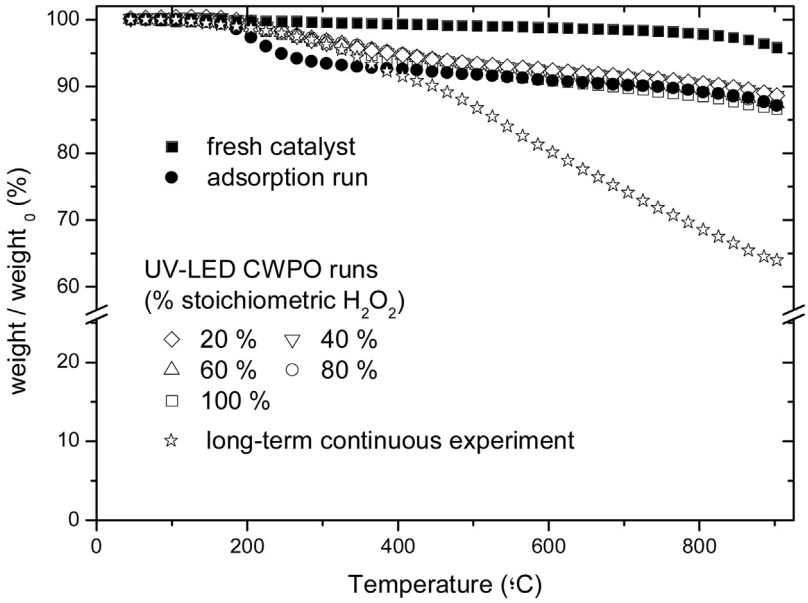

Fig. 4. N_2-TGA curves of fresh and used Fe/AC_M catalyst after adsorption, batch and long-term continuous CWPO + UV LED runs.

1 mg/L upon the inclusion of UV-LED radiation corroborating that UV-LED radiation easily decomposes oxalic acid under these conditions. Because of the lower oxalic acid concentration, the iron leaching dramatically decreased more than four-fold, from around 17% to less than 4%, without and with irradiation, respectively, thus enlarging the life cycle of the Fe/AC_M catalyst. With respect to the TOC reduction, after 180 min, oxalic, acetic and formic acids, along with non-identified compounds, are the main responsible of the residual TOC (12 mg/L) under dark conditions, whereas the residual TOC (2 mg/L) in the irradiated runs correspond to traces of formic and acetic acid together with very small amount of non-identified compounds. In both cases, the ecotoxicity of the effluent was negligible.

The other main advantage of combining both processes lies on a more efficient use of H_2O_2. It was completely decomposed after 180 min under CWPO + UV LED conditions, whereas a 5% residual concentration (that cannot be recovered and has to be eliminated before discharge due to its toxicity [26]) remains in the reaction media in absence of irradiation. To assess the H_2O_2 consumption we have defined a normalized H_2O_2 yield (ε_N), as $\varepsilon/\varepsilon_{max}$, where ε corresponds to the amount of TOC removed (expressed in mg) per unit weight of H_2O_2 fed (expressed in g) and ε_{max} is the maximum value of ε at complete TOC conversion when using the stoichiometric H_2O_2 dose (153 mg TOC/g H_2O_2 in the case of aqueous phenol solutions). Irradiating with UV-LED allowed increasing ε_N from 0.84 to 0.98 after 180 min.

3.3. Optimizing the H_2O_2 dose

A set of CWPO + UV-LED experiments were performed using different H_2O_2 doses within 20–100% of the theoretical stoichiometric amount (14 mol H_2O_2/mol phenol), following the same procedure as before. Table 2 collects the TOC removal and the concentrations of aromatics (phenol, catechol, hydroquinone and

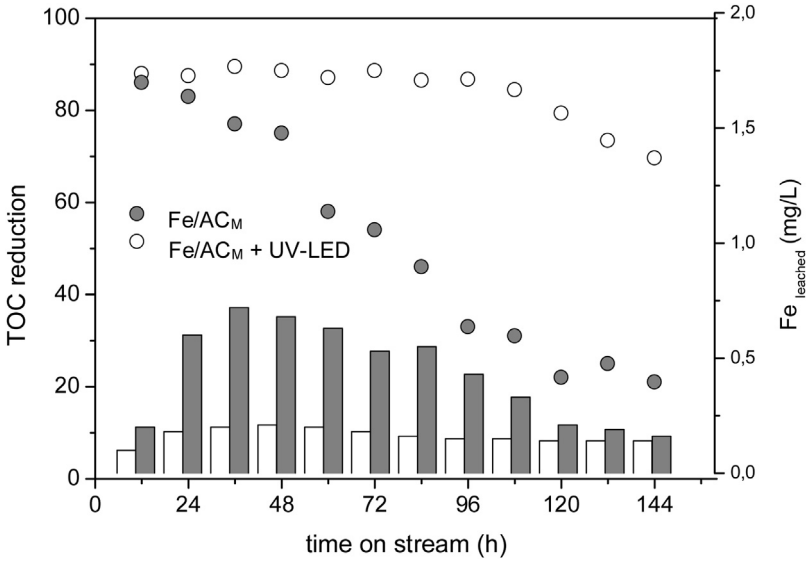

Fig. 5. TOC reduction (symbols) and Fe leached (bars) upon time on stream in the long-term continuous CWPO experiment with and without UV-LED radiation. Operating conditions $C_{phenol,0}$: 100 mg/L, $C_{H2O2,0}$: 500 mg/L, W_{cat}: 50 mg, flow rate: 0.5 mL/min, T: 50 °C and pH_0: 3.

p-benzoquinone), short organic acids (maleic, oxalic, acetic and formic) and Fe leached to the liquid after complete disappearance of the fed.

These results confirm the beneficial effect of UV-LED on CWPO, which could allow reducing the needs of H_2O_2 a critical issue in Fenton-like systems. The reduction of TOC from the aqueous phase at a H_2O_2 dose as low as 60% of the stoichiometric ratio was around 95%. Under these conditions, no aromatics were detected in the liquid and the residual TOC corresponds to short-chain organic acids, being the ecotoxicity of the effluent almost negligible.

Nevertheless, it must be noted that, due to the high adsorption capacity of activated carbon, a portion of aromatic-like compounds could remain adsorbed on the catalyst surface [6] as seems to indicate the significant reduction in the BET surface area after reaction (Table 1). To check this point, the TGA curves of used and fresh catalyst were obtained. They can be seen in Fig. 4, which includes also the TGAs of the catalyst after 180 min in contact with phenol (adsorption run) and after a long-term continuous (150 h tos) CWPO + UV-LED experiment.

The results clearly confirm the presence of some species adsorbed on the catalyst. The weight-loss percentages of the catalyst after reaction (around 10% higher than that of the fresh catalyst) were similar regardless the initial H_2O_2 concentration and comparable with that of the catalyst after the adsorption run. However, the shapes of the curves, in the 200–600 °C range show some differences. The main weight-loss percentage of the catalyst after phenol adsorption occurs in the 200–250 °C range, whereas in the catalyst after reaction that weight-loss takes places continuously within a wider range, suggesting a mix of higher molecular-weight species most probably aromatic condensation byproducts from oxidative coupling reactions.

3.4. Long-term continuous experiments

The presence of adsorbed species on the catalyst can provoke a very fast deactivation by blocking the access to the active sites. Those compounds can be easy removed from the catalyst by washing with 1 N NaOH solution, restoring almost completely the catalytic activity [6]. However performing a long-term continuous experiment is useful to learn on the activity decay upon time on stream. Fig. 5 shows the evolution of TOC and iron leached upon 150 h time on stream working at similar conditions as in the previous batch runs. As before, the results were compared with those achieved by CWPO alone (in absence of irradiation). Photolysis experiments were also carried out (data not shown), yielding TOC depletion lower than 15%.

According to the results of Fig. 5, during the first 100 h (about 30 times the hydraulic retention time), the loss of catalytic activity of Fe/AC_M under UV-LED/CWPO was negligible, showing a dramatically difference with the occurred in absence of irradiation. TOC conversion was continuously above 85%, being formic acid the main byproduct detected, along with some amounts of maleic and oxalic acid. Neither phenol nor other aromatic byproducts were detected in solution. H_2O_2 conversion within that time was close to 100%. The leaching of the active phase was always very low. The measured iron concentration in solution was below 0.2 mg/L, which contrasts with up to 0.75 mg/L in absence of radiation. After 100 h on stream the amount of iron leached was less than 25% of the initial load in the catalyst, whereas without UV-LED, that value steeply rose up to the triple. Beyond 100 h a slight but continuous loss of activity was observed. TOC conversion and H_2O_2 decomposition diminished to 75% and 90%, respectively after 150 h on stream. Besides, maleic and formic acid concentrations slightly increased. This would indicate a lower oxidation rate due to the blocking and/or the loss of active sites. The TGA curve of Fe/AC_M catalyst after 150 h on stream and the significant reduction of the BET surface area support this conclusion. As can be observed in Fig. 4, the weight-loss percentage was close to 40%, around four times higher than in batch runs. The main differences amid those TGA curves occurs beyond 400 °C, which could indicate a progressive accumulation of oligomeric condensation species on the surface of the catalyst, as a result of oxidative coupling of phenol and phenolic intermediates on the activated carbon surface [28]. It must be underlined that the total amount of those deposits on catalyst surface was around 20 mg, representing no more than 6% of the total amount of organic carbon fed to the reactor along 150 h on stream. Besides, the BET surface area decreased to 324 m^2/g that is a reduction around 65% compared with the fresh catalyst (Table 1). The micro and mesopore volume also significantly decreased from 0.38 cm^3/g and 0.12 cm^3/g to 0.09 cm^3/g and 0.05 cm^3/g, respectively, endorsing the aforementioned hypothesis.

The possible homogeneous contribution must be negligible looking at the low iron concentration in the liquid phase (<0.2 mg/L) and the scarce TOC depletion in absence of radiation where iron concentration in solution was up to four times higher. Besides, under quite similar iron concentration in solution (tos > 120 h) great differences in TOC reduction were maintained (70% *versus* 20% with and without irradiation, respectively).

4. Conclusions

The irradiation with UV LED (λ: 400–405 nm) appears a suitable solution to overcome the drawbacks associated with the use of activated carbon-supported iron catalyst in CWPO. The combined system CWPO + UV-LED (λ: 400–405 nm) allowed 95% mineralization of phenol (100 mg/L) with the stoichiometric dose of H_2O_2 at 50 °C. Oxalic acid was completely mineralized thus reducing the leaching of the active metallic phase from the catalyst, a main drawback of CWPO with activated carbon-supported iron catalysts. That combination also provides an alternative to close the Fe(II)/Fe(III) redox cycle, enhancing the HO• generation. The beneficial effect on the stability of the catalyst was checked in long-term continuous experiments where no significant loss of activity was observed upon 100 h on stream. However, beyond that time, the activity monotonically decayed, which can be attributed to the loss of active sites consequent to iron leaching as well as to their blockage by organic deposits on the surface of the catalyst most probably consisting of oligomeric condensation species from oxidative coupling of phenol and aromatic byproducts.

Acknowledgements

The authors wish to thank Ph.D. N. Menéndez for her help in Mössbauer spectroscopy. Spanish MINECO and Comunidad de Madrid have supported this work through the projects CTQ2013-41963-R and S2013/MAE-2716, respectively.

Appendix A. Supplementary data

Supplementary data associated with this article can be found, in the online version, at http://dx.doi.org/10.1016/j.apcatb.2016.04.010.

References

[1] A. Rey, A.B. Hungría, C.J. Duran-Valle, M. Faraldos, A. Bahamonde, J.A. Casas, J.J. Rodriguez, Appl. Catal. B: Environ. 181 (2016) 249–259.
[2] H.S. Park, J.R. Koduru, K.H. Choo, B. Lee, J. Hazard. Mater. 286 (2015) 315–324.
[3] S.A. Messele, O.S.G.P. Soares, J.J.M. Órfão, F. Stüber, C. Bengoa, A. Fortuny, A. Fabregat, J. Font, Appl. Catal. B: Environ. 154–155 (2014) 329–338.
[4] F. Duarte, V. Morais, F.J. Maldonado-Hódar, L. Madeira, Chem. Eng. J. 232 (2013) 34–41.

[5] F. Duarte, F.J. Maldonado-Hódar, L. Madeira, Appl. Catal. B: Environ. 103 (2011) 109–115.
[6] J.A. Zazo, J.A. Casas, A.F. Mohedano, J.J. Rodriguez, Appl. Catal. B: Environ. 65 (2006) 261–268.
[7] C.M. Domínguez, P. Ocón, A. Quintanilla, J.A. Casas, J.J. Rodriguez, Appl. Catal. B: Environ. 144 (2014) 599–606.
[8] F. Martínez, I. Pariente, C. Brebou, R. Molina, J.A. Melero, D. Bremner, D. Mantzavinos, J. Chem. Technol. Biotechnol. 89 (2014) 1182–1188.
[9] R.S. Ribeiro, A.M.T. Silva, J.L. Figueiredo, J.L. Faria, H.T. Gomes, Appl. Catal. B: Environ. 140–141 (2013) 356–362.
[10] C.M. Domínguez, P. Ocón, A. Quintanilla, J.A. Casas, J.J. Rodriguez, Appl. Catal. B: Environ. 140–141 (2013) 663–670.
[11] F. Lücking, H. Köser, M. Jank, A. Ritter, Water Res. 32 (1998) 2607–2614.
[12] A. Dhaouadi, N. Adhoum, Appl. Catal. B: Environ. 97 (2010) 227–235.
[13] V.P. Santos, M.F.R. Pereira, P.C.C. Faria, J.J.M. Órfão, J. Hazard. Mater. 162 (2009) 736–742.
[14] J.A. Zazo, A.F. Fraile, A. Rey, A. Bahamonde, J.A. Casas, J.J. Rodriguez, Catal. Today 143 (2009) 341–346.
[15] A. Rey, M. Faraldos, A. Bahamonde, J.A. Casas, J.A. Zazo, J.J. Rodriguez, Ind. Eng. Chem. Res. 47 (2008) 8166–8174.
[16] K.Y.A. Lin, F.K. Hsu, RSC Adv. 5 (2015) 50790–50800.
[17] J.C. Tristão, F.G. de Mendoça, R.M. Lago, J.D. Ardisson, Environ. Sci. Pollut. Res. 22 (2015) 856–863.
[18] J.A. Zazo, J. Bedia, C.M. Fierro, G. Pliego, J.A. Casas, J.J. Rodriguez, Catal. Today 187 (2012) 115–121.
[19] B.C. Faust, R.G. Zepp, Environ. Sci. Technol. 27 (1993) 2517–2522.
[20] Y.G. Zuo, J. Hoigne, Environ. Sci. Technol. 26 (1992) 1014–1022.
[21] G. Pliego, P. Garcia-Muñoz, J.A. Zazo, S. Diaz-Rullo, J.A. Casas, J.J. Rodriguez, ANQUE-ICCE-BIOTEC2014 Congress, Libro de Actas, pg. 277, ISBN: 978-84-697-0726-5.
[22] W. Jo, R.J. Tayade, Ind. Eng. Chem. Res. 53 (2014) 2073–2084.
[23] J.A. Zazo, G. Pliego, S. Blasco, J.A. Casas, J.J. Rodriguez, Ind. Eng. Chem. Res. 50 (2011) 866–870.
[24] R.A. Brand, Nucl. Instrum. Methods Phys. Res. B28 (1987) 398–416.
[25] G.M. Eisenberg, Ind. Eng. Chem. Anal. 15 (1943) 327–328.
[26] E.B. Sandell, Colorimetric Determination of Traces of Metals, Interscience Pubs, New York, 1959.
[27] J.A. Zazo, J.A. Casas, C.B. Molina, A. Quintanilla, J.J. Rodriguez, Environ. Sci. Technol. 41 (2007) 7164–7170.
[28] D.O. Cooney, Z. Xi, AIChE J. 40 (2) (1994) 361–364.